

Technical University of Denmark



Exchange interaction in the heavy rare earth metals calculated from energy bands

Lindgård, Per-Anker

Publication date:
1974

Document Version
Publisher's PDF, also known as Version of record

[Link back to DTU Orbit](#)

Citation (APA):
Lindgård, P-A. (1974). Exchange interaction in the heavy rare earth metals calculated from energy bands. (Risø-M; No. 1701).

DTU Library

Technical Information Center of Denmark

General rights

Copyright and moral rights for the publications made accessible in the public portal are retained by the authors and/or other copyright owners and it is a condition of accessing publications that users recognise and abide by the legal requirements associated with these rights.

- Users may download and print one copy of any publication from the public portal for the purpose of private study or research.
- You may not further distribute the material or use it for any profit-making activity or commercial gain
- You may freely distribute the URL identifying the publication in the public portal

If you believe that this document breaches copyright please contact us providing details, and we will remove access to the work immediately and investigate your claim.

Risø - M -

| | |
|---|---|
| <p>Title and author(s)</p> <p>Exchange Interaction in the Heavy Rare Earth Metals Calculated from Energy Bands by Per-Anker Lindgård</p> | <p>Date February 1974</p> <p>Department or group Physics</p> <p>Group's own registration number(s)</p> |
| <p>25 pages + 1 tables + 6 illustrations</p> | |
| <p>Abstract</p> <p>The indirect exchange interaction (RKKY) is calculated for the heavy rare earth metals. The conduction electrons are treated by the augmented-plane-wave (APW) method. Numerical results for the susceptibility χ_q for APW- and free electrons are given. The numerical accuracy is tested for the free electron model using both a root-sampling method and a linearized integral method. The first method requires 450,000 and the latter 9,000 points in the entire Brillouin zone for a good agreement with the Lindhard function. χ_q and the wave vector dependent exchange integral J_q is calculated for Gd, Tb, Dy, and Er in the ordered phase. J_q is calculated for Gd with the inclusion of the matrix element, calculated on the basis of APW functions.</p> | <p>Copies to</p> |
| <p>Available on request from the Library of the Danish Atomic Energy Commission (Atomenergikommissionens Bibliotek), Risø, DK-4000 Roskilde, Denmark Telephone: (03) 35 51 01, ext. 334, telex: 43116</p> | |

ATOMIC ENERGY COMMISSION
Research Establishment Risø

February 1974

Exchange Interaction in the Heavy Rare Earth
Metals Calculated from Energy Bands

by

Per-Anker Lindgård
Danish Atomic Energy Commission
4000 Roskilde
Denmark

ISBN 87 550 0254 4

Lectures given at XI Annual Winter School for Theoretical Physics
Karpacz, Poland 18-2 to 3-3 1974.

Contains unpublished materials. Should not be quoted or referred
to without the permission of the author.

1. INTRODUCTION

The heavy rare earth metals were obtained in pure form and as single crystals about ten years ago. This made a detailed experimental investigation possible. Neutron scattering in particular has been an important tool. As a result we by now have obtained a very complete knowledge about the magnetic interactions. The experimental facts, which are reviewed in ¹⁾, revealed that the magnetic properties are determined by an intricate interplay of forces of similar magnitude. The dominant is the indirect Ruderman-Kittel-Kasuya-Yosida (RKKY) exchange interaction, which we shall attempt to calculate from first principles, here. Of importance is also the crystal field anisotropy and magnetoelastic effects. The anisotropy of this origin is of a single ion type. Recent neutron scattering measurements ²⁾ have shown that also two-ion-anisotropy may be of importance. There are numerous possibilities for anisotropy of the interaction between the moments at different sites. As we shall see the RKKY interaction, which is mediated by the conduction electrons, is anisotropic in the magnetically ordered phase. The two-ion-interaction, which is mediated by phonons, is strongly anisotropic. The magnitude of the interaction between the spin system and the lattice is determined by the coupling between the spin- and orbital-motion of the electrons. If the spin-orbit coupling and the orbital momentum is large we must therefore expect large anisotropies both of single-ion and two-ion nature. Also the RKKY interaction becomes anisotropic as discussed by Kaplan and Lyons ³⁾.

In order to avoid the complications of anisotropy we shall start by considering the RKKY interaction in a pure spin system with no orbital effects. This is exemplified by gadolinium, which has a ⁸S ground state. The electronic configuration of a Gd atom is a xenon core with seven 4f electrons and three (5d¹6s²) outer electrons.

The basic interaction is between the localized 4f electrons belonging to the inner shells of gadolinium and the conduction electrons. Rudermann and Kittel assumed for simplicity that the conduction electrons were completely free (i.e. plane wave states). We are now able to go a step further and treat the conduction electrons in a more realistic fashion. A standard technique

is the augmented plane wave (APW) method ^{4,5}.

2. THE AUGMENTED PLANE WAVE METHOD (APW)

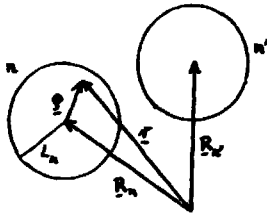
In the APW-method the electrons are supposed to move in a simplified potential which is atomic like inside a sphere (the muffin tin (in two dimensions)) around each ion and constant (=0) between the spheres. The Schrödinger equation is then solved numerically for this potential by the variational method.

The trial wave function is obtained by expanding the wave functions inside the spheres in atomic like functions and between the spheres in plane waves. The wave functions are matched at the surface of the spheres and the coefficients in the expansion is determined by minimizing the energy.

The wave function for the electrons, the crystal wave function, is therefore

$$\psi_{\underline{k},E}(\underline{r}) = \sum_i A_i(\underline{k}) \phi_{\underline{k}_i}(\underline{r}), \quad (2)$$

where the coefficients $A_i(\underline{k})$ are to be determined variationally. The sum is over a set of reciprocal lattice vectors \underline{l}_i where we write $\underline{k}_i = \underline{k} + \underline{l}_i$.



The augmented plane wave is outside the spheres

$$\phi_{\underline{k}_i}(\underline{r}) = \frac{1}{\sqrt{\Omega}} e^{i \underline{k}_i \cdot \underline{r}} \quad (2)$$

where Ω is the volume of the unit cell.

Inside the n'th sphere it is

$$\phi_{\underline{k}_i}(\underline{r}) = e^{i \underline{k}_i \cdot \underline{R}_n} \sum_{l=0}^{\infty} \sum_{m=-l}^l A_{lm}(\underline{k}) v_{l,E}(\rho) Y_{lm}(\hat{\rho}), \quad \rho = |\underline{r} - \underline{R}_n| < L_n \quad (3)$$

where L_n is the radius of the sphere and \underline{R}_n the vector to the center. The number of l values to be included in the sum are not specified at this point. However, if we want to represent s, p, d or f character of the crystal wave function we must include $l=0,1,2,3$. The wave function in the two regions (2) and (3) can be made to match at the sphere surface by choosing the expansion coefficients $A_{lm}(\underline{k})$ in (3). By expanding (2) in spherical harmonics and Bessel functions around the center of the sphere

$$\frac{1}{\sqrt{\Omega}} e^{i \underline{k} \cdot \underline{r}} = \frac{4\pi}{\sqrt{\Omega}} e^{i \underline{k}_i \cdot \underline{R}_n} \sum_{l=0}^{\infty} \sum_{m=-l}^l i^l j_l(k\rho) Y_{lm}^*(\hat{k}_i) Y_{lm}(\hat{\rho}) \quad (4)$$

and equating this with (3) at $\rho=L_n$ we find

$$A_{lm}(\underline{k}) = \frac{4\pi}{\sqrt{\Omega}} e^{i \underline{k}_i \cdot \underline{R}_n} i^l Y_{lm}^*(\hat{k}_i) j_l(kL_n) / v_{l,E}(L_n) \quad (5)$$

The APW function $\phi_{\underline{k}_i}(\underline{r})$ with this $A_{lm}(\underline{k})$ is called a basis function. It is continuous, but has a discontinuous slope at the sphere radius. The expansion coefficients $A_i(\underline{k})$ in (1) are found by minimizing the energy

$$E_{\underline{k}} = \langle \psi_{\underline{k}} | H | \psi_{\underline{k}} \rangle / \langle \psi_{\underline{k}} | \psi_{\underline{k}} \rangle \quad (6)$$

This gives a secular equation for the determination of the $A_i(\underline{k})$. We shall not go further into this.

The $v_{l,E}(\rho)$ functions are the radial solution to the Schrödinger equation inside the sphere

$$\left(\frac{1}{r^2} \frac{d}{dr} \left(r^2 \frac{d}{dr} \right) + \frac{l(l+1)}{r^2} + V(r) - E' \right) v_{l,E}(r) = 0 \quad (7)$$

$v_{l,E}(\rho)$ must be regular at the center ($\rho=0$), but there is no

boundary condition at $\rho = \infty$ and hence there exist solutions for all E' . This is a complication and E' must be chosen self-consistently according to (6). Several methods have been devised to make this practically. Harmon⁵⁾ used a linearized AWP method⁶⁾ to obtain the wavefunctions for Gd, which we are going to use later. Also the crystal potential inside the sphere, $V(r)$, must be chosen selfconsistently. This is done by summing the contribution to the Coulomb potential from a large number of surrounding ions including the conduction electron charge density. The exchange interaction may be included in the Slater $\rho^{1/3}$ approximation.

By carrying out this programme we are able to find a set of selfconsistent energy bands $E_{\mathbf{k}}$ and the corresponding wave functions $\psi_{\mathbf{k}}$ for the conduction electrons. The variationally determined wavefunctions are presumably less reliable than the energies. Also they are more sensitive to the approximation made when constructing the muffin-tin-potential. However, we may expect them to be best near the atoms inside the spheres. Therefore they should be quite adequate in calculating the matrix element between the conduction electrons and the localized 4f electrons, which is relevant for the calculation for the RKKY interaction. The 4f electrons are well approximated by the atomic wavefunctions of Herman and Skillman⁷⁾.

3. THE RKKY-INTERACTION WITH REALISTIC ENERGY BANDS

3.1. The Interaction between conduction electrons and the 4f electrons

By means of these realistic energy bands and wave functions we can proceed to calculate the RKKY interaction.¹⁸⁾

In the calculation of the energy bands we did not consider explicitly the interaction between two electrons but rather the interaction between one electron and the average potential for all the other electrons. As a perturbation on this model we shall now consider the interaction between a conduction electron and a 4f electron. The direct interaction is the Coulomb interaction $v(\mathbf{r}_1 - \mathbf{r}_2) = \frac{e^2}{|\mathbf{r}_1 - \mathbf{r}_2|}$ between a conduction electron at \mathbf{r}_1

and a 4f electron at \mathbf{r}_2 . In general, however, the potential is screened by the presence of the other electrons, in which case $v(\mathbf{r}_1 - \mathbf{r}_2)$ will be modified to for example the Yukawa potential $e^2 \exp(-\kappa|\mathbf{r}_1 - \mathbf{r}_2|)/|\mathbf{r}_1 - \mathbf{r}_2|$, where κ^{-1} is the screening length.

Since we are interested in the magnetic interaction we shall only consider the exchange interaction and further only the term which involve the scattering of a conduction electron on a 4f electron.

This is represented in terms of electron creation and annihilation operators, $c_{\mathbf{k}}^{\dagger}$ and $c_{\mathbf{k}}$ respectively as follows

$$v(\mathbf{r}_1 - \mathbf{r}_2) = \frac{1}{4} \sum_{\substack{\mathbf{k}_i s_i \\ i=1,2,3,4}} \langle k_4 s_4, k_3 s_3 | v(\mathbf{r}_1 - \mathbf{r}_2) | k_2 s_2, k_1 s_1 \rangle \\ c_{k_4 s_4}^{\dagger} c_{k_3 s_3}^{\dagger} c_{k_2 s_2} c_{k_1 s_1} \quad (8)$$

where $\langle v |$ is the matrix element, k_i the crystal momentum and s_i the spin index. Since $v(\mathbf{r}_1 - \mathbf{r}_2)$ is independent of spin, the spin must be conserved in the scattering process. Let us assume that the 4f electrons are well approximated by localized atomic states $\psi_{4f}(\mathbf{r} - \mathbf{R}_n)$ at the site \mathbf{R}_n and the conduction electron wave function is $\psi_{\mathbf{k}, E}(\mathbf{r})$ in (1). Then the conduction electrons are scattered from one state of momentum \mathbf{k} to another of \mathbf{k}' whereas the localised electrons are scattered from one localised state to another, with or without spin flip. We can represent the change in the localised states by the change in the total local spin S_n instead of by means of the creation and annihilation operators in (8).

The perturbation of the single electron Hamiltonian which was used in the band calculation is therefore in this approximation for the s-f exchange interaction as follows

$$H_{sf}(\mathbf{R}_n) = -\frac{1}{N} \sum_{\mathbf{k}, \mathbf{k}'} j_{sf}(\mathbf{k}, \mathbf{k}') e^{i(\mathbf{k} - \mathbf{k}') \cdot \mathbf{R}_n} \\ \{ (c_{\mathbf{k}\uparrow}^{\dagger} c_{\mathbf{k}'\uparrow} - c_{\mathbf{k}\downarrow}^{\dagger} c_{\mathbf{k}'\downarrow}) S_n^z \\ + c_{\mathbf{k}\uparrow}^{\dagger} c_{\mathbf{k}'\downarrow} S_n^- + c_{\mathbf{k}\downarrow}^{\dagger} c_{\mathbf{k}'\uparrow} S_n^+ \}$$

where the last line shows the spin flip scattering processes and the middle line the processes without spin flip.

The matrix element is

$$j_{sf}(k, k') = N \int d\underline{r}_1 d\underline{r}_2 \{ \phi_{4f}^*(\underline{r}_1 - \underline{R}_n) \psi_k^*(\underline{r}_2) v(\underline{r}_1 - \underline{r}_2) \phi_{4f}(\underline{r}_2 - \underline{R}_n) \psi_k(\underline{r}_1) \} e^{i(k' - k) \cdot \underline{R}_n} \quad (10)$$

$j_{sf}(k, k')$ is independent of the lattice site \underline{R}_n since

$$\psi_k(\underline{r}) = u_k(\underline{r}) e^{i\mathbf{k}\cdot\underline{r}} = \psi_k(\underline{r} - \underline{R}_n) = u_k(\underline{r}) e^{i\mathbf{k}\cdot\underline{r}} e^{-i\mathbf{k}\cdot\underline{R}_n} \quad (11)$$

according to Bloch's theorem. We shall assume that $\phi_{4f}(\underline{r} - \underline{R}_n)$ vanishes outside the muffin-tin-sphere around \underline{R}_n and therefore we only integrate (10) inside the sphere to obtain the generalized exchange integral $j_{sf}(k, k')$.

3.2. The effect of orbital moment of the 4f electrons

Let us generalize the interaction Hamiltonian (9) slightly. In the presence of orbital momentum L for the 4f electrons the total angular momentum $\underline{J} = \underline{L} + \underline{S}$ ($J = |L \pm S|$ since \underline{L} and \underline{S} are parallel, with + for the heavy and - for the light rare earth metals). Then we can replace \underline{S} in (9) by the spin projection along \underline{J} namely $(g-1)\underline{J}$, where g is the Landé factor. A proper calculation of the orbital effects will give rise to a more complicated form for (9) as discussed by Kaplan and Lyons³). The effect is however small and will be neglected here.

3.3. The effect of magnetic ordering of the localized moments

If the localized moments are ordered throughout the crystal they will give rise to a molecular magnetic field H_M which will shift the energy of the otherwise degenerate spin-up and spin-down electrons i.e. $E_{k,\uparrow} \pm E_{k,\downarrow}$. This molecular field model is equivalent to the rigid-band-shift model. The shift in energies can be calculated exactly by diagonalizing the single electron Hamiltonian and the molecular field term

$$H = \sum_{k,s} E_{k,s} c_{k,s}^\dagger c_{k,s} + H_M \quad (10)$$

The molecular field is obtained by taking the thermal average value of localized moments S_n in (9).

For the sake of generality we shall calculate the RKKY interaction for the conically ordered phase. The cone-structure, which contains as special cases both the ferromagnetic and the spiral structure, is defined by the following parameterization of the ionic moments:

$$\langle \underline{S}_{R_n} \rangle = m(T) S \{ \sin\theta \cos(Q \cdot \underline{R}_n), \sin\theta \sin(Q \cdot \underline{R}_n), \cos\theta \} \quad (11)$$

where $m(T)$ is the temperature dependent reduced magnetization, θ is the cone angle and Q the spiral vector.

Using (9) and (10) we find the molecular field H_M to be used in (10), which then can be diagonalized using standard techniques.

We find the new energies

$$e_{k,Q}^\pm = e_D \pm \sqrt{(\epsilon_m - \Delta)^2 + \gamma^2} \quad (12)$$

where

$$e_D = (E_{k-Q/2} \pm E_{k+Q/2})/2 \quad (13)$$

$$\Delta = S m(T) \cos\theta j_{sf}(k, k) \text{ and } \gamma = S m(T) \sin\theta j_{sf}(k, k+Q)$$

the new wave functions are

$$\psi_{k,+} = \cos\phi |k-Q/2, \uparrow\rangle + \sin\phi |k+Q/2, \downarrow\rangle \quad (14)$$

$$\psi_{k,-} = -\sin\phi |k-Q/2, \uparrow\rangle + \cos\phi |k+Q/2, \downarrow\rangle$$

where

$$\tan\phi = \frac{\gamma}{e_{k,Q}^\pm + \Delta - E_{k-Q/2}} \quad (15)$$

(12) shows the energies of the conduction electrons in the magnetically ordered phase.

For the ferromagnetic case $\theta=0$ and $Q=0$ and we find the rigid band model:

$$\epsilon_{\mathbf{k}}^{\pm} = E_{\mathbf{k}} \pm \Delta \quad (16)$$

where Δ goes to zero when the magnetization vanishes at T_c .

For the spiral case we obtain the results discussed by Elliott and Wedgwood⁸). In this case, as in the general case of cone structure, the magnetic order produces gaps in the electron energy bands related to the spiral vector Q . This is of importance when calculating the temperature dependence of the spiral vector $Q(T)$, and in general the temperature dependence of the exchange interaction.

The magnetic order, the effect of which we have just included, is of course a consequence of the interaction between the local moments. In other words the interaction must be calculated self-consistently.

3.4. The generalized RKKY interaction in the ordered phase

We now proceed to calculate the RKKY interaction by taking into account the terms left in (9). $H_{sf} - H_M$ is not diagonal between the states (12), but the effect thereof can be found by second order perturbation theory.

The shift in energy is then using (9) and (12):

$$\delta E^{(2)} = \sum_{n,n'} \sum_i \langle 0 | H_{sf}(R_n) - H_M | i \rangle \langle i | H_{sf}(R_{n'}) - H_M | 0 \rangle / (\epsilon_0 - \epsilon_i) \quad (17)$$

where $|0\rangle$, $|i\rangle$ are the initial and intermediate states respectively and ϵ_0 , ϵ_i the corresponding energies, from (12). We must remember that the electrons can be scattered only from an occupied state to an empty state according to the Pauli principle. This can be accounted for by the fermi factors $f_k = [e^{(E_k - \epsilon_F)/kT} + 1]^{-1}$. We shall assume that f_k is a step function, being 1 for energies smaller than the fermi energy and 0 for larger energies.⁹) We then find from (17) for the cone-structure the following effective interaction between the localized moments.

$$H_q = -J_q^n S_q^z S_q^z - \frac{1}{2} J_q^{\pm} (S_q^+ S_{-q} + S_q^- S_{-q}^+) \quad (18)$$

where the wave vector dependent exchange interaction is

$$J_q^n S_q^z S_{-q}^z = \sum_{nn'} S_n^z S_{n'}^z e^{iQ(R_n - R_{n'})} \frac{1}{2N} \sum_k f_k (1 - f_{k+q}) |j_{sf}(k, k+q)|^2 \left[(1 + \cos^2 2\phi) \left\{ \frac{1}{\epsilon_k^+ - \epsilon_{k+q}^+} + \frac{1}{\epsilon_k^- - \epsilon_{k+q}^-} \right\} + \sin^2 2\phi \left\{ \frac{1}{\epsilon_k^+ - \epsilon_{k+q}^-} + \frac{1}{\epsilon_k^- - \epsilon_{k+q}^+} \right\} \right]$$

and (19)

$$J_q^{\pm} (S_q^+ S_{-q}^- + S_q^- S_{-q}^+) = \sum_{nn'} e^{iQ(R_n - R_{n'})} \{ S_n^+ S_{n'}^- e^{iQ(R_n - R_{n'})} + S_n^- S_{n'}^+ e^{-iQ(R_n - R_{n'})} \} \frac{1}{2N} \sum_k f_k (1 - f_{k+q}) |j_{sf}^*(k, k+Q+q) j_{sf}(k, k-Q+q)| \left[\sin^2 2\phi \left\{ \frac{1}{\epsilon_k^+ - \epsilon_{k+q}^+} + \frac{1}{\epsilon_k^- - \epsilon_{k+q}^-} \right\} + (1 + \cos^2 2\phi) \left\{ \frac{1}{\epsilon_k^+ - \epsilon_{k+q}^-} + \frac{1}{\epsilon_k^- - \epsilon_{k+q}^+} \right\} \right]$$

For a ferromagnetic ordering is $\phi=0=Q=0$ from (13,15) and (19) reduces considerably. We find

$$J_q^n = \frac{1}{N} \sum_k f_k (1 - f_{k+q}) |j_{sf}(k, k+q)|^2 \left\{ \frac{1}{\epsilon_k^+ - \epsilon_{k+q}^+} + \frac{1}{\epsilon_k^- - \epsilon_{k+q}^-} \right\} \quad (20)$$

and

$$J_q^{\pm} = \frac{1}{N} \sum_k f_k (1 - f_{k+q}) |j_{sf}(k, k+q)|^2 \left\{ \frac{1}{\epsilon_k^+ - \epsilon_{k+q}^+} + \frac{1}{\epsilon_k^- - \epsilon_{k+q}^-} \right\}$$

where ϵ_k^{\pm} are given by (16).

This interaction is anisotropic contrary to the paramagnetic RKKY-interaction. For the ferromagnetic phase we obtain a J_q'' and a J_q^+ for the spin components parallel or perpendicular to the average moment direction. J_q'' involves only scattering of electrons with no spin-flip and J_q^+ only with spin-flip. J_q'' can be measured directly by spin wave measurements, whereas J_q^+ cannot be measured as a function of the wave vector. However, the magnetic contribution to the free energy is $-J_q'' S_q^z S_q^z$ for $q=0$. If J_q'' has a maximum for $q \neq 0$ it shows that, if for no other reasons, a non-ferromagnetic state would have lower free energy. However it is necessary to calculate selfconsistently the energy difference between the various phases.

3.5. The magnitude of the s-f interaction

Experimental information about the magnitude of the s-f interaction $j_{sf}(k, k')$ can be obtained directly by considering the polarization of the conduction electrons. This can be found either by measuring the total moment pr. atom or by means of NMR technique measuring the magnetic field, which the conduction electrons create at the nucleus.

For ferromagnetic ordering the net polarization is given by the difference between the number of electrons with spin up and spin down. In the rigid band model ($T=0$) this is to a good approximation

$$n_{\uparrow} - n_{\downarrow} = (\Delta_{\uparrow} - \Delta_{\downarrow}) \rho(E_F) / 2 = \Delta \rho(E_F) = S m(T) \frac{1}{N} \sum_k j_{sf}(k, k) \rho(E_F), \quad (21)$$

where $\Delta_{\uparrow, \downarrow}$ is the energy shift of the spin up and spin down electrons relative to the paramagnetic fermi-energy E_F and $\rho(E_F)$ is the density of states at the fermi energy. We obtained (21) by averaging over all momenta in (10).

Since each unpaired electron contributes to the magnetic moment by $\frac{1}{2} g_B \mu_B = 1 \mu_B$ we find for the average s-f interaction ($m(0)=1$)

$$j_{sf}(0) = \frac{\Delta}{S} = \frac{2 \delta M}{g_B \mu_B S \rho(E_F)}$$

where δM is the conduction electron polarization in μ_B and $g_B=2$.

From magnetization data¹⁾ and a theory for the temperature dependence of the magnetization,¹⁰⁾ we find the results given in table 1.

| | J | L | S | g | $\rho(E_F)$ | States Ryd | E_F Ryd | $\delta M \mu_B$ | Δ Ryd | $j_{sf}(0) (\delta M)$ | $j_{sf}(0) (T_C)$ |
|----|-------|-----|-----|---|-------------|---------------|-----------|------------------|--------------|------------------------|-------------------|
| Gd | 7/20 | 7/2 | 2 | | 25.6 | | .440 | .55 | .021 | .006 | .006 |
| Th | 6/3 | 3 | 3/2 | | 28.0 | | .509 | .41 | .015 | .005 | .006 |
| Dy | 15/25 | 5/2 | 4/3 | | 27.7 | | .513 | .41 | .015 | .006 | .007 |
| Er | 15/26 | 3/2 | 6/5 | | 23.0 | | .451 | .22 | .010 | .006 | .009 |

Table 1: Data for the heavy rare earth metals, $\rho(E_F)$ is the calculated density of states, Δ is half the ferromagnetic splitting and $j_{sf}(0)$, the deduced s-f interaction in Ryd. We notice it is almost independent of the elements. The values estimated from the ferromagnetic transition temperature is given in the last column.

The s-f interaction can be estimated from the ferromagnetic transition temperature as follows

$$k T_C = 0.792 \frac{1}{2} J_0'' J(J+1) \quad (22)$$

where $J_0'' = [(g-1) j_{sf}(0)]^2 \rho(E_F)$.

0.792 is a factor which corrects the molecular field value for T_C .

Having derived the expressions (19) and (20) for the indirect exchange interaction and estimated the interaction strength we shall consider the actual calculation. The summation over the wave vectors \underline{k} in (19) and (20) must be done numerically.

4. NUMERICAL METHODS

On the basis of the APW energy bands calculated by Louks¹¹⁾ we can evaluate the sums in (19) and (20). The matrix element $j_{sf}(k, k+q)$ must be evaluated using the wave functions. The major contribution to the sum comes when the denominator is small. In other words when the electrons are scattered from just below to just above the fermi surface. This makes the numerical calculation difficult. A possible way is to sum over a very large number of k points and exclude the contribution when the denominator is smaller than a chosen number δ . This is called the root-sampling method. This is a brute-force principal value calculation (correct in mathematical sense, if we let δ go to zero). However, it is very difficult to test the convergence of this procedure numerically. In fact the noise in the computer sets a limit for how small δ can be chosen and how fine a mesh of k point we can use - apart from the practical problem of the increasing computer time. However, the method is simple and was used by Liu et al¹²⁾ and also in several of the results to be discussed.¹³⁾ The convergence seems to be good and the computing time reasonable with a mesh with 450 060 points in the total Brillouin zone. These calculations were simplified by the assumption that the matrix element $j_{sf}(k, k+q)$ was independent of k and only dependent on the difference q , i.e. $j_{sf}(k, k+q) \approx j_{sf}(q)$.

In order to test the convergence and also to make it feasible to include a k dependence of $j_{sf}(k, k+q)$ a different numerical method was used. In this method the Brillouin zone is divided into a relatively small number of micro cells. Inside each cell are the constant energy surfaces ϵ_k approximated by planes. This makes it possible to integrate analytically inside each micro cell. The integrals are only divergent if the energy surfaces ϵ_k and ϵ_{k+q} are exactly parallel. This will occur very rarely. This so-called linearized method was developed for density of state calculations by Gilat and Raubenheimer¹²⁾ and was later simplified by Jepsen and Andersen, who used it for calculating fermi surface areas. The sum in (19) and (20) are more complicated and has not previously been calculated using this method. We shall therefore briefly describe it. The Brillouin zone is divided into micro cells of the shape of tetrahedra¹⁵⁾ of a

volume V as shown on fig. 1. In each corner are the energies

$$\epsilon_k^i = \epsilon_1, \epsilon_2, \epsilon_3, \epsilon_4 \text{ and } \epsilon_{k+q}^i = \epsilon_1, \epsilon_2, \epsilon_3, \epsilon_4$$

Since the constant energy surfaces are approximated by planes the constant energy difference $\omega = \epsilon - \epsilon$ is also a plane. The problem is therefore to integrate

$$I = \int_{\omega_{\min}}^{\omega_{\max}} \frac{1}{\omega} A(\omega) d\omega \quad (23)$$

over the part P of the tetrahedra for which $\epsilon < E_F$ and $\epsilon > E_F$, where the area of the constant energy difference plane inside P is $A(\omega)$. P may be a complicated polyhedra because of the restrictions coming from the fermi f_k factors in (19) and (20). $f_k(1-f_{k+q})$ can by symmetry considerations be replaced by $\frac{1}{2}(f_k - f_{k+q})$. We do not use the latter form (although it simplifies the calculation considerably) because the result then is given as the difference between two large numbers which may be inaccurate numerically. For illustration we shall consider the case where the condition ($\epsilon < E_F$ and $\epsilon > E_F$) is fulfilled for the whole tetrahedra.

The area $A(\omega)$ is then simply the area of a cut of the tetrahedra perpendicular to the ω planes. This area is clearly a quadratic function of ω , being zero for ω outside the range $\omega_{\max} - \omega_{\min}$. The area can easily be expressed by geometrical considerations in terms of the corner energies ϵ^i and ϵ^i and V , it is not necessary to calculate the normal vector to the ω planes. Therefore, in the case where we must integrate over the whole tetrahedra (23) is simply

$$I = \int_n \int_{\omega_{\min}}^{\omega_{\max}} \{a_n(\epsilon^i \epsilon^i) + b_n(\epsilon^i \epsilon^i)\omega + c_n(\epsilon^i \epsilon^i)\omega^2\} / \omega d\omega, \quad (24)$$

where the sum is over each type of cross sections (triangle or square) and a_n, b_n, c_n the parameters characterizing this. We notice that the integral is logarithmically divergent when $\omega_{\min} = \omega_{\max}$ i.e. when the planes of ϵ_k and ϵ_{k+q} are parallel.

We can test the method on the free electron model where the energy bands are parabolic. The sum (19,20) can then be integrated exactly giving the Lindhard function. The result of the root-

sampling method and the linearized method is shown on fig. 2 together with the exact result. We see that the linearized method gives an excellent result for only 9 000 k-points in the entire Brillouin zone.

5. RESULTS

Let us start by considering what effect the magnetic ordering has on the RKKY exchange interaction. That is the same as asking what is the intrinsic temperature dependence. The formulas were developed in (15) and (20). We shall only be interested in a qualitative answer, which will show the general magnitude and the direction of the effects. We therefore make the simplifying assumption that for this purpose we can consider the matrix element $j_{sf}(k, k+q)$ to only depend on the difference q . Our problem then reduces to calculating the electronic static susceptibility.

$$\chi_q^{\alpha\beta} \sim \frac{1}{N} \sum_k f_k (1 - f_{k+q}) / (e_k^\alpha - e_{k+q}^\beta)$$

We determine the matrix element $|j_{sf}(q)|^2$ from experiments, by comparing $\chi_q^{\frac{1}{2}}$, the calculated sum without it, with the $J_q^{\frac{1}{2}}$ obtained from spin wave measurements. The matrix element is assumed to be insensitive to the magnetic structure and is used in obtaining the exchange interaction in other magnetic phases. The absolute scale of $J_q^{\frac{1}{2}}$ cannot be determined from the spin waves. The scale is found from the transition temperature T_N and coincidentally from the conduction electron polarization table 1. This gives J_q^n for $q=0$.

Fig. 3 shows the results for the ferromagnetic phase at $T=0$ for Gd, Tb, Dy, and Er using the APW energy bands and the root-sampling method with 450 000 points in the entire Brillouin-zone (the linearized method was also used as a test, it gave essentially the identical result and is not shown). It is clear that J_q^n and $J_q^{\frac{1}{2}}$ differ significantly for all materials. The dots show the points compared with the experimental $J_q^{\frac{1}{2}}$; the calculation was done for 50 equidistant q -values. For terbium the experimental $J_q^{\frac{1}{2}}$ shows no maximum for $q \neq 0$, whereas the calculated J_q^n shows that Tb

has a tendency to form a spiral structure even in the ferromagnetic phase. The enhancement of the maximum for $q \neq 0$ is also evident for Dy and Er in which the spiral region is large. The opposite effect occurs for Gd, where J_q^n shows that Gd should not form a spiral phase, and nor it does. Furthermore it is clear that the maxima in J_q^n occurs at q -values very close to the experimental spiral vectors (indicated with an arrow) and that it is significantly displaced from the peaks in $\chi(q)$, which is directly related to the presence of flat parallel pieces of Fermi surface. The matrix element thus plays an important role in determining the wave vector dependence of the exchange interaction. The semiempirically found wave vector dependence of the matrix element is very similar for all materials, despite the rather different $\chi(q)$ functions. This is encouraging for the present analysis. Overhauser¹⁶⁾ has argued that the matrix element should follow the $4f$ -form factor. By extending his model to include the Bloch character of the conduction electrons we would expect a narrow central peak originating from the conduction electrons. This is the form found in fig. 4.

The energy difference between the ferromagnetic and spiral phases is, as judged from the $T=0$ ferromagnetic data fig. 4, for Gd, Tb, Dy, and Er in per cent of the exchange energy: -14%, +5%, +5%, +12%. This gives for Tb, Dy, and Er a stabilization of the spiral phase by 10 K/ion times the reduced magnetization squared. The magnetoelastic stabilization of the ferromagnetic phase is for these materials at the ferromagnetic-spiral transition typically 1 K/ion.

The last column in fig. 4 shows a calculation at half the saturation moment of $\chi_0^n(q)$ in the ferromagnetic phase and $\chi_0^{\frac{1}{2}}(q)$ in the spiral phase, with spiral vector Q . The contribution to the free energy is proportional to $-|j(q)|^2 \chi_0^{\frac{1}{2}}(0) \cdot \chi_0^{\frac{1}{2}}(0)$ as a function of the spiral vector Q follows closely that of $\chi_0^n(q)$ as a function of q , which shows that the most probable spiral vector coincide with that found in the ferromagnetic phase. The precise location is sensitive to the wave vector dependence of the matrix element.

The above simple calculation gave encouraging results and is a natural extension of the calculation of the exchange interaction in the paramagnetic phase.¹²⁾ However, the next step is

to consider the matrix element more seriously. We shall do this for the paramagnetic phase with no band splitting. Harmon⁵⁾ has by means of the APW functions calculated $|j_{sf}(\underline{k}, \underline{k}+\underline{q})|^2$ for the simplest material Gd. A few of the matrix elements are shown on fig. 3. They generally show the \underline{q} dependence we anticipated, namely a sharp peak at $q=0$. On the other hand it is clear that they are quite sensitive to the value of \underline{k} , and irregularities occur as a function of \underline{q} , which presumably comes from the hybridization of the p- and d-wave functions.

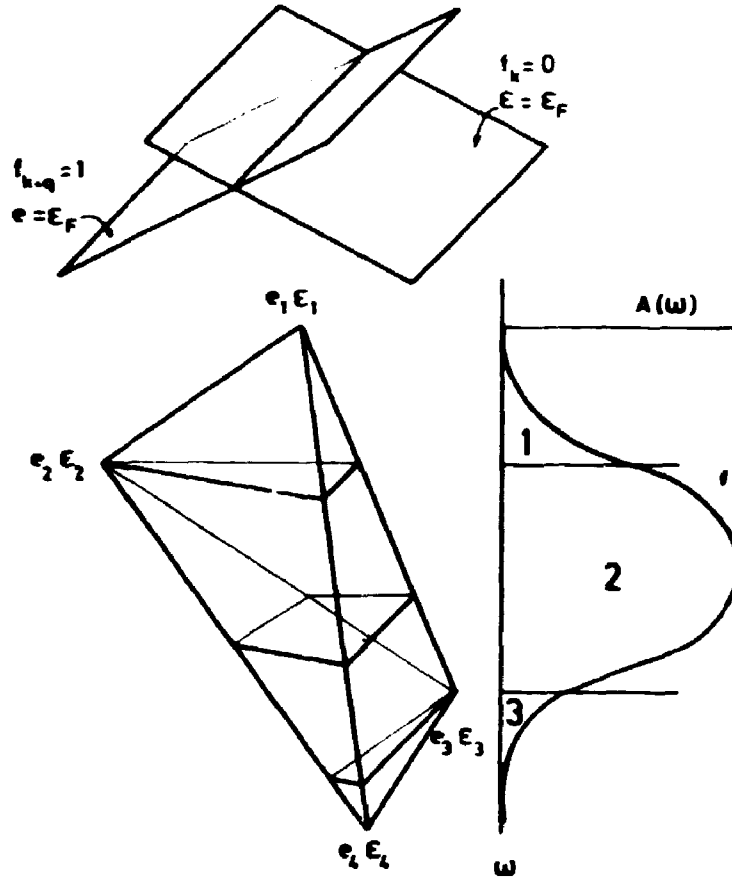
It is therefore of importance to carry out the complete sum (20) including the \underline{k} dependence of $j_{sf}(\underline{k}, \underline{k}+\underline{q})$. Preliminary results are shown on fig. 5. The calculation is performed by the linearized-integral method (23) with 7000 \underline{k} points in the entire Brillouin zone and with $j_{sf}(\underline{k}, \underline{k}+\underline{q})$ included rectangularly at 1250 \underline{k} points. The result is the first direct calculation of the RKKY interaction for Gd with no adjustable parameters. The \underline{q} -dependence of $J_{\underline{q}}$ is in satisfactory agreement with that obtained experimentally from spin wave measurements, shown as $J_{\underline{q}}^1$ in fig. 4. An important question to be investigated is if the major contribution to $J_{\underline{q}}$ comes from the part of the sum for which $j_{sf}(\underline{k}, \underline{k}+\underline{q})$ is insensitive to \underline{k} or if both the \underline{k} and \underline{q} dependence are equally important, the last case would indicate that the matrix element is as important in determining the magnetic properties of the heavy rare earths as the fermi surface topology.

Work on these questions is in progress. A large number of problems are waiting to be done in developing and refining the theory, here presented, and confronting it with the experimental facts.

REFERENCES

- 1) R.J. Elliott ad., Magnetic Properties of Rare Earth Metals (Plenum Press, London, 1972)
- 2) J.G. Houman, J. Jensen, P. Touborg (1974) to be published
- 3) J.A. Kaplan and D.H. Lyons, Phys. Rev., 129, 2072 (1963)
- 4) T.L. Louks, Augmented Plane Wave Method (W.A. Benjamin, Inc., New York, 1967)
- 5) B.M. Harmon, Conduction Electron Polarization, Spin Densities and The Neutron Magnetic Formfactor of Gadolinium. Thesis (1973)
- 6) D.D. Koelling, J. Phys. Chem. Sol. 33, 1335 (1972)
- 7) F. Herman and S. Skillman, Atomic Structure Calculations, Prentice-Hall, Inc. Englewood Cliffs, New Jersey (1963).
- 8) R.J. Elliott and F.A. Wedgwood, Proc. Phys. Soc., 81, 846 (1963)
- 9) This is a very good approximation at all relevant temperatures.
- 10) P.A. Lindgård and O. Danielsen (1974) (to be published)
- 11) S.C. Keeton and T.L. Louks, Phys. Rev. 168, 672 (1968)
- 12) S.H. Liu, R.P. Gupta, S.K. Sinha, Phys. Rev. B, 4, 1100 (1971)
- 13) P.A. Lindgård and S.H. Liu, Proceeding of the Int. Conf. on Magnetism, Moscow (1973).
- 14) G. Gilat and L.J. Raubenheimer, Phys. Rev., 144, 390 (1966)
- 15) O. Jepsen and O.K. Andersen, Solid State Commun., 9, 1763 (1971)
- 16) A.W. Overhauser, J. Appl. Phys., 34, 1019 (1963)
- 17) W.E. Evenson and S.H. Liu, Phys. Rev., 178, 783 (1968)
- 18) We follow closely the notation of A.J. Freeman ref. 1.

LINEARIZED INTEGRAL METHOD



$$\frac{1}{N} \sum_k \frac{f_k(1-f_{k+q})}{\epsilon_k - \epsilon_{k+q}} \quad \begin{array}{l} \epsilon = \epsilon_k \quad e = \epsilon_{k+q} \\ \omega = \epsilon_k - \epsilon_{k+q} \end{array}$$

$$\sum_n \int_{\omega_{min}}^{\omega_{max}} A_n(\omega)/\omega d\omega$$

Fig. 1 At the top is shown the constant energy plane, for $\epsilon_k = \epsilon_F$ and $\epsilon_{k+q} = \epsilon_F$. The Brillouin zone is divided into tetrahedra as shown below of constant volume V , here oriented so that the direction of increasing energy difference ω is vertical. The cut with the constant ω planes are shown. The area of these cuts are quadratic functions of ω in the regions 1, 2 and 3. The sum then reduces to the integral shown in the lowest line. In general the plane $\epsilon_k = \epsilon_F$ and $\epsilon_{k+q} = \epsilon_F$ may also cut the tetrahedra. In this case must only be integrated over the part P for which the $f_k(1-f_{k+q})$ condition is fulfilled.

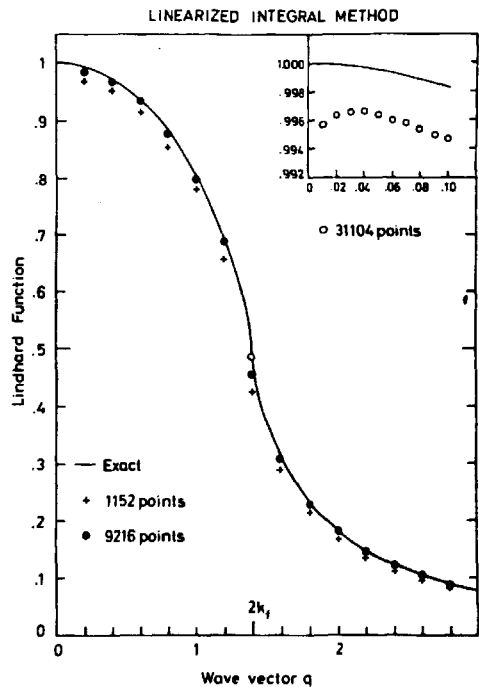


Fig. 2a The generalized susceptibility for free electrons. The points are the numerical results for the linearized-integral-method for meshes with 1000, 9000 and 30000 points in the entire Brillouin zone (hcp) with $k_F=0.7$ of the zoneboundary wavevector ($\Gamma-K$). We notice a very good agreement with the theoretical Lindhard function already with the mesh with 9000 points. The insert shows that the most difficult region for $q \rightarrow 0$ is reproduced well. The systematic deviation is due to the fact that the integration is performed in the inscribed polyhedra in the fermi sphere. It has both convex and concave parts and the volume is better approximated by the polyhedra in a realistic system.

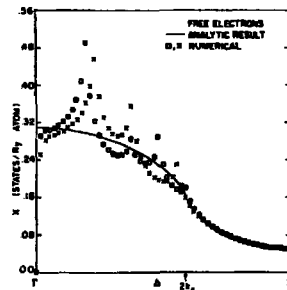


FIG. 4. Generalized susceptibility for three-dimensional free electrons.

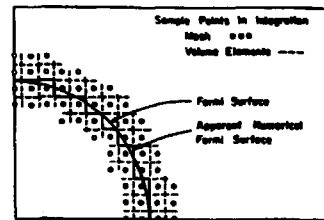


FIG. 2. Example of distortion of the Fermi surface in the numerical calculation due to the finite mesh size.

Fig. 2b The result of the root-sampling-method¹⁷⁾ in a coarse mesh of 27000 points. We notice that spurious peaks occur because of the mesh for k values less than $2k_F$. The convergence is good in a mesh with 450000 points, not shown.^{12,13)}

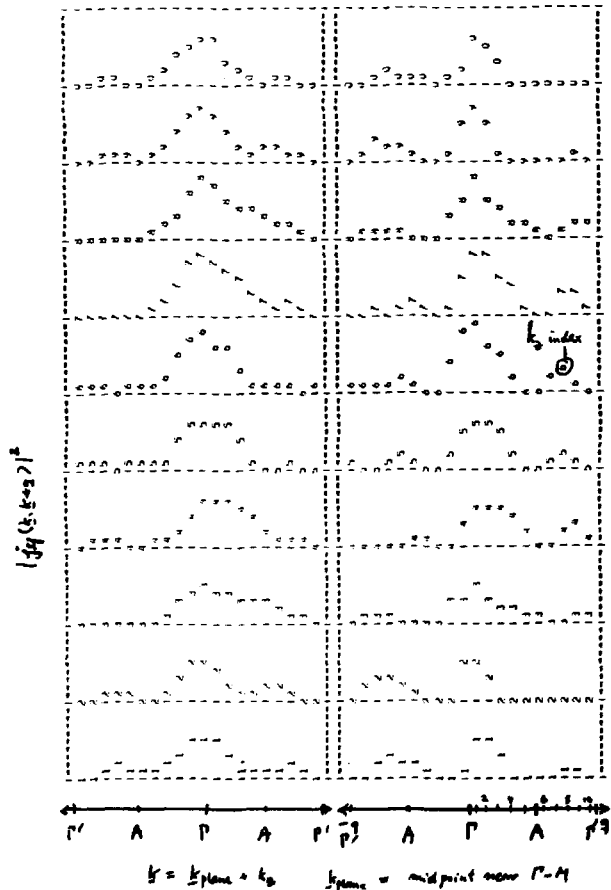


Fig. 3 Example of $|j_{\perp f}(k, k+q)|^2$ for Gd calculated by the APW method by Harmon.⁵⁾

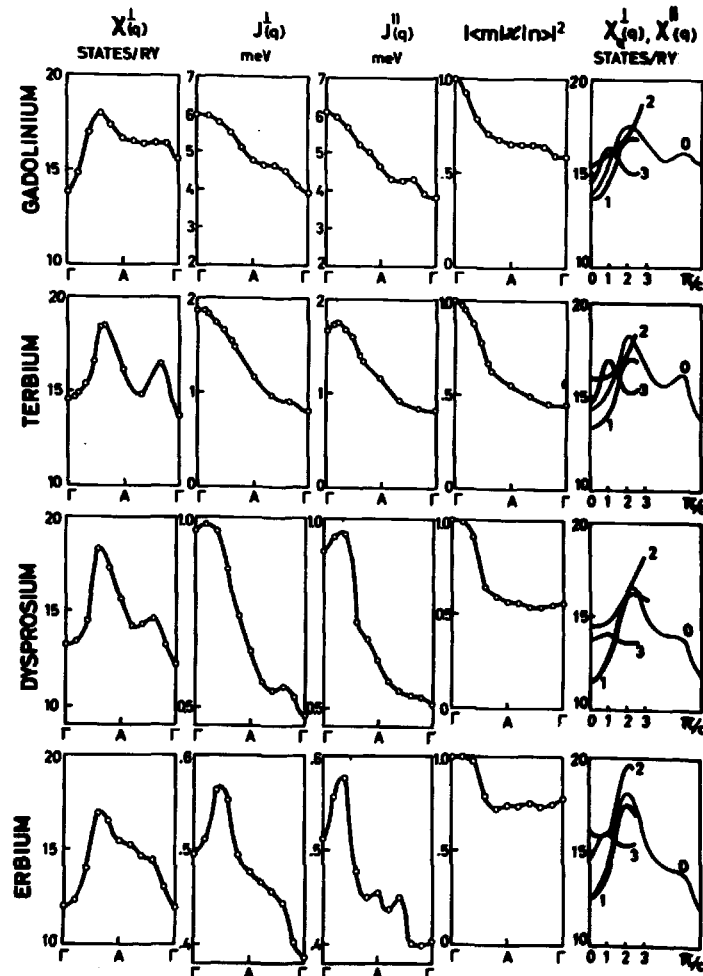


Fig. 4. The perpendicular susceptibility $\chi_{\perp}^I(q)$, the perpendicular experimental exchange interaction $J_{\perp}^I(q)$, the calculated parallel exchange interaction $J_{\parallel}^{II}(q)$ and the deduced matrix element $|j(q)|^2/|j(0)|^2 = |\langle m | \chi | n \rangle|^2$ for the ferromagnetic phase (splitting: 0.008 Ryd). The last column shows $\chi_{\perp}^I(q)$ in the spiral phase for $Q_0 = 0$, $Q_1 = \frac{1}{6} \frac{\pi}{c}$, $Q_2 = \frac{2}{6} \frac{\pi}{c}$ and $Q_3 = \frac{3}{6} \frac{\pi}{c}$ (splitting 0.004 Ryd); the corresponding ferromagnetic $\chi_{\parallel}^{II}(q)$ is also shown (thin line).

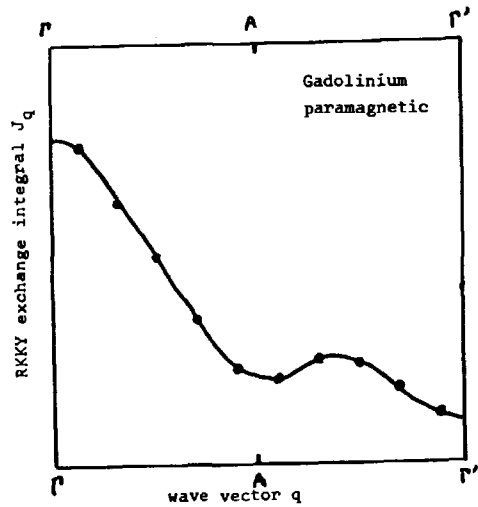


Fig. 5. Preliminary result for the calculated RKKY interaction, using Harmon's APW matrix element⁵⁾. Only scattering relevant for an extended zone has been included as a first approximation.

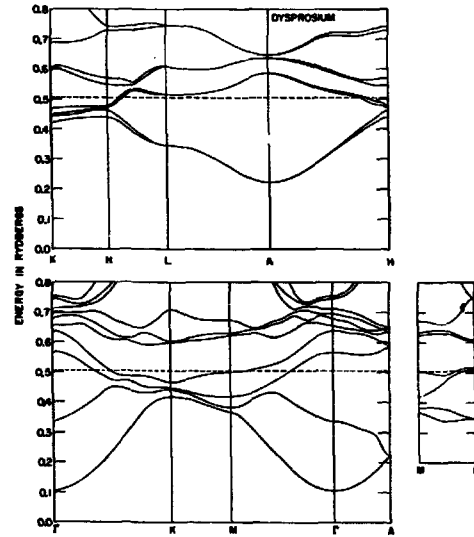


Fig. 6. APW energy bands for Dy^{11} . Only the bands crossing the Fermi surface have been included in the sum.